ELSEVIER

Coordination Chemistry Reviews
190–192 (1999) 127–153

COORDINATION CHEMISTRY REVIEWS

www.elsevier.com/locate/ccr

The structure of cobalt corrinoids based on molecular mechanics and NOE-restrained molecular mechanics and dynamics simulations☆

Helder M. Marques [a,*], Kenneth L. Brown [b]

[a] *Centre for Molecular Design, Department of Chemistry, University of the Witwatersrand, Johannesburg, South Africa*
[b] *Department of Chemistry, Ohio University, Athens, OH, USA*

Accepted 17 February 1999

Contents

Abstract

Approaches the authors have used for modeling the structure of the cobalt corrins by molecular mechanics methods are reviewed. A parameter set for use with the MM2 force field has been developed. The structure of the corrins is well reproduced, and the force field

☆ Based on a paper presented at the 33rd ICCC, Florence, Italy, August 30–September 4, 1998.

* Corresponding author. Fax: +27-11-339-7967.
E-mail address: hmarques@aurum.chem.wits.ac.za (H.M. Marques)

010-8545/99/$ - see front matter
PII: S0010-8545(99)00074-0

has been validated by predicting novel structures and subsequently verifying the predictions by X-ray structure determination. The force field has been useful in relating details of the structures of alkylcobalamins to the lability of the Co–C bond towards bond homolysis, probing the conformational flexibility of the 5′-deoxyadenosyl ligand in adenosylcobalamin (AdoCbl, coenzyme B_{12}), and studying the conformation of coenzymatically active AdoCbl analogs, including one that fails to crystallize. The technique has been further extended to include the use of NMR-derived distance restraints in molecular dynamics (MD) and simulated annealing (SA) procedures. This methodology permits for the first time a detailed description of the motions of cobalt corrins in solution. The consensus structures of SA calculations agree well with the known solid state structures of two complete cobalamins (CH_3Cbl and CNCbl), including, importantly, the corrin fold angle. The base-off analogs have significantly smaller corrin fold angles, implying that base-on Cbls are under steric strain. These observations lend credence to proposals for the enzymatic labilization of the Co–C bond involving upward flexing of the corrin ring. Preliminary results on the modeling of coenzyme B_{12} (AdoCbl) in solution are reported.

Keywords: Cobalt corrins; Distance restraints; Molecular dynamics; Molecular mechanics; Molecular modelling; Vitamin B_{12}

1. Introduction

Molecular mechanics (MM) is a computational technique firmly rooted in the concepts of a classical mechanics description of molecular structure [1,2]. The focus is on the motion of the nuclei and electron density is not explicitly taken into account. A molecule is treated as a set of interacting atoms and the consequences of all possible pairwise interactions between the atoms describes a potential energy hypersurface. Minima on this surface correspond to stable molecular conformations, and the overall or global minimum to the most stable conformation. Whilst well-established as a technique for describing the structure of small organic molecules, it is only relatively recently that the technique has found application in inorganic chemistry (see for example [3–10]).

The inter-atomic interactions are described by a number of components such as bond lengths (r), valence angles (θ), dihedrals (χ), non-bonded interactions, out-of-plane deformations and electrostatic interactions. Each component is treated by means of a potential energy function and the total strain energy, E_{str}, of the system is the sum of the contribution from each factor (Eq. (1)). Each structural parameter, p, has an ideal or strain-free value, p°. When the system is subjected to a deformation, a restoring force, usually taken to be harmonic in nature, operates (Eq. (2)). The force constant, k_p, is a measure of the resistance of p to the deformation. The strain energy, E_p, is the integral of Eq. (2). The collection of potential energy functions, E_p, the p° values and the associated force constants, k_p, constitute the MM force field.

$$E_{\mathrm{str}} = \sum E_r + \sum E_\theta + \sum E_\chi + \sum E_{nbd} + \sum E_{oop} + \sum E_{elec} + \ldots\ldots \quad (1)$$

$$F = -\frac{\partial E}{\partial p} = k_p(p - p^\circ) \quad (2)$$

$$E_p = \frac{1}{2} k_p(p - p^\circ)^2 \quad (3)$$

Harmonic potentials, or variations thereof, are often used to treat the first two terms of Eq. (1), while the other terms are usually handled by special methods. For example, dihedrals are treated by a Fourier expansion of the torsional angle, θ; van der Waals interactions are often modeled either with the Lennard–Jones or the Buckingham potential; and electrostatic interactions are handled either with a Coulomb's law expression between point charges, or between all pairs of dipoles that are not attached to the same atom [11–19].

In this paper we review the use of MM methods for exploring the structure of the cobalt corrinoids, derivatives of vitamin B_{12} (cyanocobalamin, CNCbl, Fig. 1). Two cobalamin coenzymes are known. Adenosylcobalamin (AdoCbl) is the cofactor in enzymes which catalyze 1,2 rearrangements of organic substrates (Scheme 1A) and the reduction of the C–2′ of the ribose of ribonucleotide triphosphates [20,21] (Scheme 1B). Methylcobalamin (CH_3Cbl) is responsible for the transfer of methyl groups; the CH_3Cbl-dependent methyltransferase enzyme systems are involved in the biosynthesis of methionine [22–24], in the regulation of tetrahydrofolate [25], in bacteria that reduce carbon dioxide to methane [26] and in anaerobes that convert carbon dioxide to acetate [27].

2. Deriving a force field for the cobalt corrinoids

Two distinct methods are currently employed to model coordination compounds using MM methods. Firstly, some generalised force fields have been developed in attempts to model as wide a range of coordination compounds as possible. These include the universal force field (UFF) of Rappé and co-workers [28], the SHAPES force field of Allured, Kelley and Landis [29] and Comba's MOMEC force field [30]. Alternatively, it is recognized that many of the fragments of coordination compounds are organic; hence a standard force field for modeling organic compounds, such as MM2/MM3 [11–13], is used as the starting point. Parameters are then developed to model the coordination sphere of the metal ion; because of the polarizing effect of the metal ion, standard 'organic' parameters may not be adequate for reproducing the structure of a ligand [31] and new atom types and parameters may have to be defined.

Even within the latter procedure, different approaches have emerged. In one, the L–M–L angular interactions are treated with a 'points-on-a-sphere' model [32,33], the computational analog of the well-established VSEPR model, by specifically taking into account 1,3 van der Waals interactions between the ligand donor atoms (see for example [34–36]); 1,3 van der Waals interactions are usually excluded in

MM force fields, being subsumed into the angle bending terms. In another approach, the metal ion is treated as any other atom, and strain- free values for the L–M–L bond angles and a force constants for angle bending are specifically developed [37–45]. We [46] have used the latter approach for extending the parameter set in a modified version [42] of MM2 [12] for the cobalt corrinoids. More recently [47], the parameter set has been revised for use with the HYPERCHEM suite of programs [48].

The development of the force field was based on 19 reported cobalt corrinoid crystal structures chosen from the structures in the Cambridge Structural Database (January 1992). Atoms were grouped into classes and the statistics on class-equivalent bond lengths and bond angles were calculated. Differences between the classes were checked for statistical significance, and the number of atom classes reduced as far as possible. The parametrization of the force field began by setting the

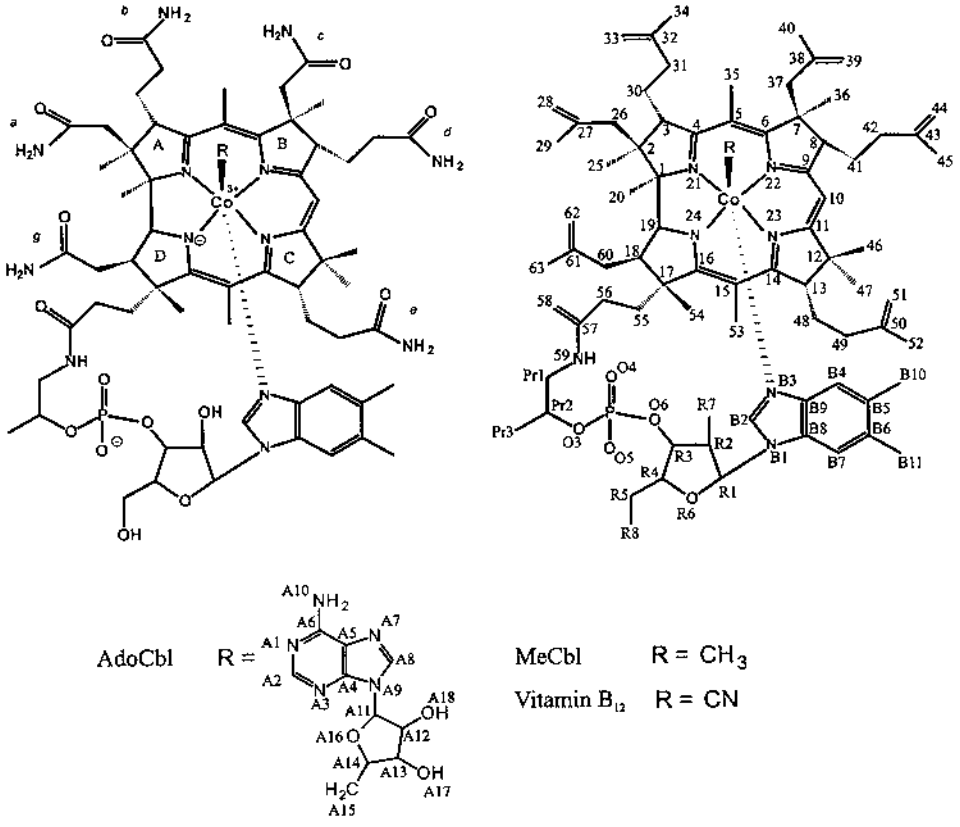

Fig. 1. The structure of the cobalamins. The standard numbering is given in the diagram on the top right. Vitamin B_{12} itself has R = CN in the upper or β coordination site. In the two coenzyme forms, R = 5′-deoxyadenosyl (adenosylcobalamin, AdoCbl) or R = Me (methylcobalamin, CH_3Cbl). Cobinamides lack the nucleotide side chain and, in aqueous solution, the lower or α coordination site is often assumed to be occupied by a water molecule.

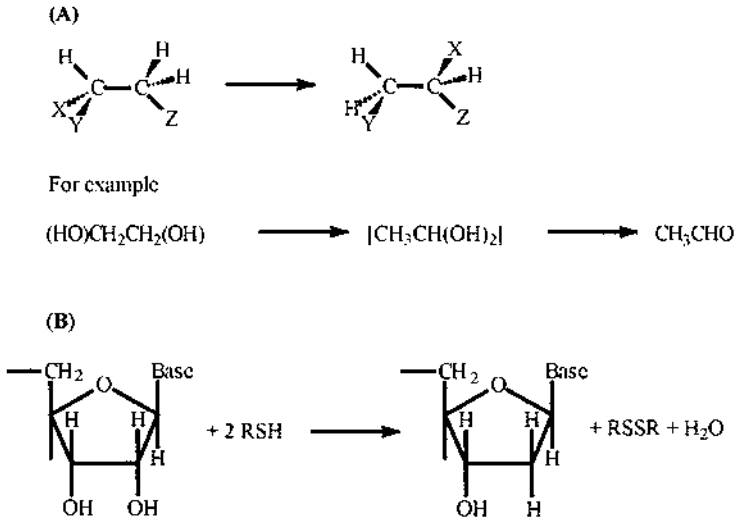

Scheme 1.

strain-free bond lengths and bond angles to the crystallographically observed means; the initial values of the force constants were determined by analogy with standard MM2 parameters, or those from other force fields for metal-containing macrocyclic systems. The structural parameters of the energy-minimized structure were compared with the crystallographic mean values and the force constants adjusted by trial and error until a best fit to the crystallographic data was obtained. The model reproduced bond lengths within 0.01 Å of the crystallographic mean, and bond angles and torsional angles within 2.4 and 4.2°, respectively; these are within the standard deviation of the mean of these parameters found within the solid state. Deviations of less than 0.02 Å, 3 and 5°, respectively, between modeled and observed bond lengths, bond angles, and torsional angles are taken to indicate a good fit [28,43].

A force field that does little else than reproduce known structures is of limited usefulness. However, before a force field can be used to predict novel structures, or to explore details of known structures, an extensive validation procedure is required. Typically, the force field is tested for its ability to reproduce known features of the class of compounds for which it has been developed and, more rigorously, to reproduce structures of related compounds not used in the derivation of the force field, or entirely new compounds (but in the same class as those used in the parametrization of the force field). It has to be accepted that a force field is designed to reproduce *average* structures and it would be unrealistic to expect every aspect of any particular structure to be reproduced. It is sufficient and fair to expect the overall features to be correctly predicted.

We demonstrated that the force field for the cobalt corrinoids correctly predicted the limited rotational flexibility of the coordinated 5,6-dimethylbenzimidazole (bzm) base, and the likely orientations of the acetamide and propionamide side chains [46]. When the *d* side chain at C8 and the *e* side chain at C13 are epimerized from the lower to the upper face of the corrin ring, the so-called *epi*Cbls are produced. A crystal structure of cyano-13-*epi*Cbl [49] was available at the time the force field was developed (a new structure, very similar to the original one, has subsequently been reported [50]); the structure was deliberately not used in the derivation of the force field. A model of the structure predicted by the force field as part of the validation procedure was found to be rather similar to the crystal structure, with some minor differences in the conformation of the C ring [46] (Fig. 2A). The MM-predicted structure of the then-unknown cyano-8-*epi*Cbl had the *d* side chain in an equatorial position. This prediction was subsequently verified experimentally when the crystal structure became available [51] (Fig. 2B).

Using MM we were able to verify the 2D-NMR observations made by Bax, Marzilli and Summers [52] that cross peaks in the spectrum of AdoCbl were inconsistent with the orientation of the adenosyl ligand observed in the solid state where the adenine ring system lies nearly parallel to the corrin ring and is located over the 'southern' quadrant of the molecule when viewed from above. They proposed a two-state model in which the Ado ligand is not only in the usual 'southern' conformation, but also, having undergone a clockwise rotation of some 50°, is in an 'eastern' conformation. By rotating the Ado ligand around the corrin ring we discovered four energy minima (Fig. 3). The global minimum is indeed the crystallographically-observed 'southern' conformation but small energy barriers exist to the 'eastern' and to a 'northern' conformation; a much larger barrier exists to a 'western' conformation. The population of both a 'southern' and an 'eastern' conformation by AdoCbl in solution at room temperature appears likely.

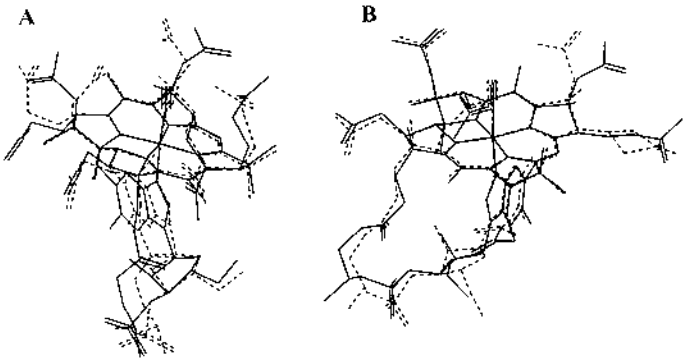

Fig. 2. The MM-predicted (——) and crystal structures (-----) of (A), cyano-13-*epi*-cobalamin and (B), cyano-8-*epi*-cobalamin overlaid at the four corrin N atoms and the cobalt ion. The MM modeling correctly predicts the disposition of the epimerized *e* and *d* side chains in the two structures, respectively. The major differences between the predicted and the observed structures are in the orientation of the other side chains of the corrin ring.

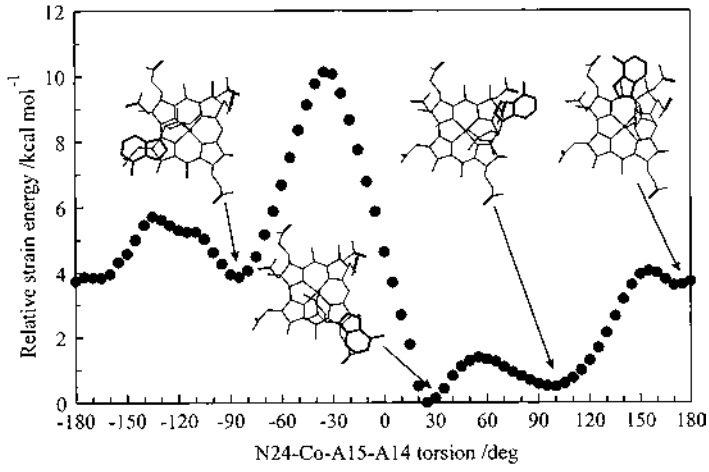

Fig. 3. Locally-minimum energy structures of adenosylcobalamin as discovered by molecular mechanics methods. The global minimum (the 'southern' conformation) is the one observed crystallographically.

With these demonstrations of its capabilities, the force field was subsequently used in a number of investigations.

3. Some examples of predictions using the force field.

3.1. Alkylcobalamins and the influence of structure on Co–C thermal bond homolysis

The structures of alkylcobalamins (RCbls) and organocobaloximes (compounds containing the Co(III)-bis(dimethylglyoximato) moiety, relevant to B_{12} chemistry because of the many parallels between the properties of their organometallic complexes and the alkylcobalamins [53]) were used to develop parameters for modeling the Co–C bond length and the Co–C–C bond angle [47,54]. The orientation of the side-chains in methyl-, adenosyl-, benzyl- and neopentylcobalamin was explored and a set of accessible conformations identified. A Boltzmann distribution was applied to these, and population-weighted values of the Co–C bond length and Co–C–X (X = C, H) bond angle determined (Table 1). As expected, the steric demands of the four alkyl ligands increase in the series Me < Bz ca. Ado < Np as determined from the values of the Co–C bond length and Co–C–X bond angle. There is an inverse relationship between the Co–C bond dissociation energy and the steric strain on the alkyl moiety, although the bond dissociation energy of BzCbl is anomalously low because of resonance stabilization of the emerging $PhCH_2^{\bullet}$ fragment.

Thus, coordination of an alkyl ligand to the metal leads to steric strain, manifest as an elongation of the Co–C bond length and the distortion of the Co–C–X bond

Table 1
Geometry of coordinated alkyl groups in alkylcobalamins determined by molecular mechanics calculations

Compound	Co–C bond length (Å)		Co–C–C bond angle (°)		Co–C–H bond angle (°)		Co–C bond dissociation energy (kcal mol^{-1}[a]
	Calculated	Observed	Calculated	Observed	Calculated	Observed	
CH3Cbl	1.988(6)	1.99(1)[b]			110.1(1)		37(3)[f]
AdoCbl	2.023(20)	2.03(2)[c]	121.6(1.5)	125[c]	104.5(3.2)	104[e]	30(2)[g]
			1.98–2.04d	121–124[d]			32(2)[h]
BzCbl	2.018(16)		117.0(3.1)		104.4(1.3)		23(1)[i]
NpCbl	2.171(7)		136.7(1.9)		92.1(1.9)		24.1(3)[j]

[a] Details of calculations are given in Ref. [54].
[b] Ref. [55].
[c] Ref. [56].
[d] Ref. [57].
[e] Ref. [57], neutron diffraction study.
[f] Refs. [58,59].
[g] Ref. [70].
[h] Ref. [60].
[i] Ref. [61]
[j] Ref. [62].

angle. Calculations show [54] that this strain is relieved, or partially relieved, as the transition state is approached. It is conceivable, therefore, that the labilization of the Co–C bond, a key feature of the AdoCbl-dependent enzymatic reactions (see below), could be achieved, as has been suggested [63–66], by the enzymatic distortion of the Co–C–C bond angle or the stretching of the Co–C bond, perhaps by an upward flexing of the corrin ring [67–69].

3.2. Side chain rotational motion and Co–C thermal bond homolysis

It is generally agreed that the first step of the AdoCbl-dependent enzymatic reactions is homolysis of the Co–C bond to produce Co(II) and an Ado$^{\cdot}$ radical, a process that is catalysed by the enzyme by 9–12 orders of magnitude [70]. Because $t_{1/2}$ for the uncatalysed reaction is inconveniently long (17 h at 85°C), neopentylcobalamin (NpCbl, $t_{1/2} = 89$ min at 25°C) has often been used as a model system [61,62,67,71–73]. The rate of thermolysis of NpCbl is measured in the presence of O_2 or a radical trap such as 4-hydroxy-2,2,6,6-tetramethylpiperidinyloxy (HTEMPO) which prevents the recombination of Co(II) and the Np$^{\bullet}$ radical. Corrections to the observed rate constants are made for the base-on/base-off equilibrium of the nucleotide loop of NpCbl (the base-off species is less reactive than the base-on species [61,74,75]), and activation parameters can be determined for the thermolysis of NpCbl: $H^{\ddagger} = 28.3$ Å, 0.2 kcal mol^{-1} and $S^{\ddagger} = 19.3$ Å 0.6 cal mol^{-1} K^{-1}.

As the positive entropy of activation is large for a reaction which involves no charge separation and a single new degree of freedom is incipient in the transition state, an hypothesis was advanced that the upwardly-projecting acetamide side chains (*a*, *c*, *g*) have their rotational freedom restricted by the coordinated alkyl ligand; in the transition state, the increased Co···C bond separation would decrease the steric interaction between the side chains and the alkyl ligand, leading directly to an increase in entropy. A number of NpCbl derivatives with altered *c* side chains, viz., NpCbl-*c*-COO$^-$, NpCbl-*c*-NHMe, NpCbl-*c*-NMe$_2$ and NpCbl-*c*-NH^{i}Pr were prepared [76] and the activation parameters for Co–C bond homolysis determined (Table 2). The value of $\Delta H^{\ddagger}$ hardly varies across the series, whereas $\Delta S^{\ddagger}$ increases with the steric bulk of the *c* side chain (but is virtually identical for the two bulkiest analogues).

The effect of the rotation of the *c* side chain about the C7–C37 bond (through 360° in steps of 10°) was investigated by MM calculations. For each step of the rotation the structure was fully energy-minimised and the Co–C bond length, and the Co–C–C and Co–C–H bond angles determined. These were found not to change significantly either by the rotation or by the bulk of the *c* side chain, in agreement with the experimental observation that $\Delta H^{\ddagger}$ remains essentially constant for the series of compounds. Relative strain energies, *E*, defined as the difference in strain energy at a given value of the C6–C7–C37–C38 dihedral angle, ω_1, used to drive the side chain rotation, and the strain energy minimum in the rotation of the *c* side chain ($\omega_1 = \pm 180°$, where the side chain points outward from the coordinated alkyl ligand), were plotted as a function of ω_1 (Fig. 4A shows an example for

Table 2
Activation parameters for the thermolysis of NpCbl and its side chain modified analogues, and molecular mechanics results

Compound	$H^{\ddagger a}$ (kcal mol^{-1})	$S^{\ddagger a}$ (cal mol^{-1} K^{-1})	Van der Waals volume of *c* side chain substituent (Å3)	E_{str} [b] (kcal deg mol^{-1})	Co–C[c] (Å)	Co–C–C[d] (°)	Co–C–H (°)
NpCbl-*c*-COO^-	27.5(1)	16.4(4)	48.5	365	2.068(5)	131.9(2)	101.2(1.4) 101.1(1.7)
NpCbl	28.3(2)	19.3(6)	58.2	395	2.068(6)	132.0(3)	101.1(1.7) 103.3(1.4)
NpCbl-*c*-NHMe	28.7(2)	21.1(7)	82.7	407	2.069(6)	132.4(4)	101.0(1.5) 102.6(1.5)
NpCbl-*c*-NMe2	29.4(2)	24.8(6)	106.2	459	2.069(7)	132.0(3)	100.8(1.8) 103.2(1.5)
NpCbl-*c*-NH^iPr	29.1(1)	24.9(3)	130.4	546	2.068(7)	131.9(2)	101.1(1.5) 103.4(1.3)

[a] For the base-on form of NpCbl.
[b] Difference in integrated strain energy, E_{str}, for the NpCbl analogue and the corresponding CH_3Cbl analogue.
[c] Average Co–C bond length for the 36 rotational positions of the *c* side chain investigated.
[d] Average Co–C–H bond angle for the 36 rotational positions of the *c* side chain investigated.

NpCbl-*c*-NH^{i}Pr); the integrated strain energy, E_{str}, was determined by numeric integration of the area under the curve. The strain energy profiles shows three maxima (the side chain passing over the C36 methyl at ω_1 ca. $-120°$; contact with coordinated Np, ω_1 ca. 0°; contact with C8H, ω_1 ca. 100°) and three minima (ω_1 ca. $-70°$, where the side chain is over the C5 region of the molecule; ω_1 ca. 60°, and the side chain is over C10; ω_1 ca. 180°, with the side chain pointing directly outwards from the corrin). To isolate the barrier due only to interaction with the Np ligand, the calculations were repeated for the CH_3Cbl-*c*-COOX analogues (Fig. 4A), and the difference taken (Fig. 4B). The differential integrated strain energy, ΔE_{str}, thus represents the additional steric strain upon rotation of the *c* side chain imposed by the Np ligand compared to the smaller CH_3 ligand. The values are listed in Table 2.

ΔE_{str} values increase with the steric bulk of the *c* side chain substituent, while the Co–C bond length and the Co–C–X (X = C, H) bond angles hardly vary. This is in line with the kinetic results: the values of $\Delta H^{\ddagger}$ are virtually invariant (there is a spread of 1.6 kcal mol^{-1}), whereas the values of $\Delta S^{\ddagger}$ are much more sensitive to side chain bulk (the spread is 8.5 cal mol^{-1} K^{-1}). This is interpreted to mean that as the steric bulk of the *c* side chain substituent increases, the steric restriction on the side chain motion increases as well which lowers the entropy of the ground

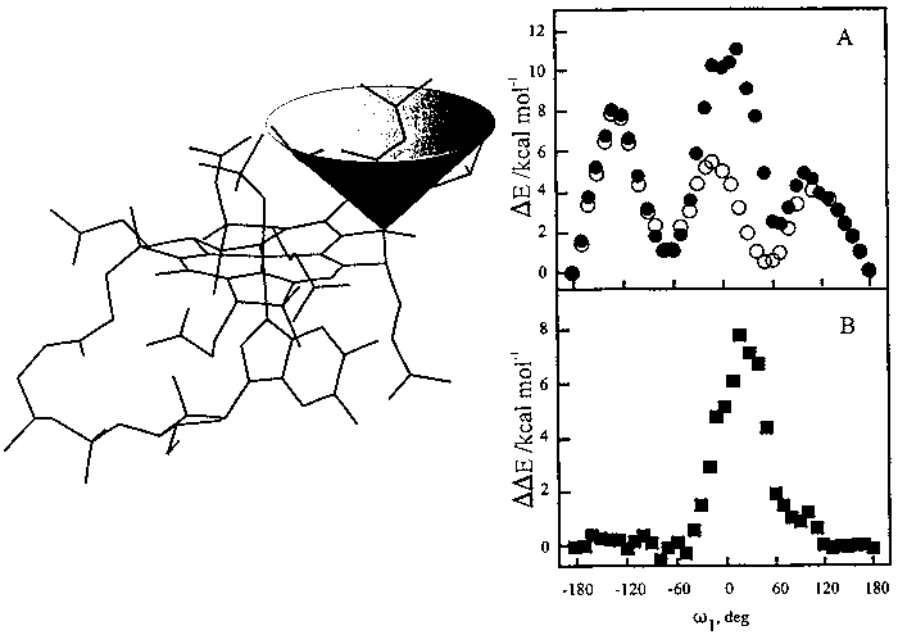

Fig. 4. Rotation of the *c* side chain of NpCbl and its energy consequences. (A) Plot of the relative strain energy, ΔE, for NpCbl-*c*-NH^{i}Pr (●) and for CH_3Cbl-*c*-NH^{i}Pr (○) as a function of the C6–C7–C37–C38 dihedral angle (ω_1). (B) Plot of the differential relative strain energy *E* between NpCbl-*c*-NH^{i}Pr and CH_3Cbl-*c*- NH^{i}Pr vs. ω_1.

state. The effect saturates, however. Presumably, once the steric bulk reaches a certain value, the side chain is precluded from visiting conformations towards the interior of the corrin, and adding further bulk has no particular effect.

When the calculations are repeated at increasing Co–C bond length (to simulate the separation of the two moieties as the transition state is approached), it is found that as the Co–C bond is stretched beyond about 3 Å, the steric contact between the Np group and the *c* side chain decreases rapidly. If it is assumed that the Co···C distance in the transition state is about 1.6 that of the ground state [77] then ΔE_{str} would be halved, decreasing by about 200 kcal deg mol^{-1}, of the same order as the difference in ΔE_{str} between the compounds with the least and most bulky *c* side chains. The separation of the alkyl ligand from the metal centre as the transition state is approached is therefore expected to substantially increase the entropy of the complex. Other investigations with Np-13-*epi*Cbl, in which the *e* side chain is epimerized from the lower to the upper face of the corrin ring, and with a NpCbl derivative referred to as NpCbl-8-butanamide where a rearrangement of the B ring leaves no substituent at C7, an upwardly-projecting methyl at C8, and the *d* side chain has been expanded by one C atom to a butanamide [78] have confirmed that side-chain motions play an important role in the entropic labilisation of the Co–C of NpCbls towards homolysis.

3.3. The structure of adenosylcobalamin in solution

One of the attractions of MM methods is that a reliable force field can be used to examine a variety of questions, including questions that explore novel ideas about the structure of compounds. Our predictions (Fig. 3) that in addition to the well-characterized 'southern' and the putative 'eastern' conformations of AdoCbl, 'northern' and 'western' conformations exist prompted us to explore the structure of AdoCbl in solution. This is important if the activation parameters for enzyme-catalyzed Co–C bond homolysis in AdoCbl are to be compared with results for protein-free species [79] since values for the latter are determined at temperatures (85–110°C) where conformations other than the 'southern' and 'eastern' conformations are likely to become accessible. The Co–C bond dissociation energy is very sensitive to the Co–C and Co–C–C geometry (Table 1) and these structural parameters may vary among the four AdoCbl conformers; hence a direct comparison may be inappropriate.

Twelve crosspeaks between protons on the Ado ligand and protons elsewhere on the molecule were observed in the rotating-frame Overhauser enhancement (ROESY) spectra of AdoCbl at 27°C. The MM energy-minimized structures were used to measure inter-proton distances and all nOe's could be attributed to H—H interactions in the 'southern' or 'eastern' conformations, or both. However, at 60°C, 27 crosspeaks were observed; assuming that these could not arise from pairs of protons separated by more than ca. 4.5 Å, 8 were compatible only with the 'northern' or 'western' conformations, or both. Therefore all four conformations of AdoCbl are accessible in solution even at 60°C. A Boltzmann distribution among all discovered conformations of the 'southern', 'eastern', 'northern' and 'western'

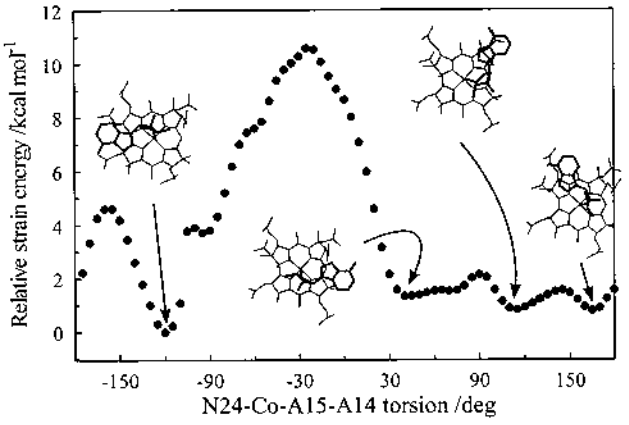

Fig. 5. The four locally minimum energy conformations of Ado-13-epiCbl as determined by MM calculations. The 'southern' conformation of the molecule is destabilized and the global minimum is predicted to be a 'western' conformation. The relatively-modest barriers between all four conformations leads to a conformationally-flexible molecule, in agreement with the many nOe's found between Ado and non-Ado proton in 2D-NMR experiments at room temperature.

conformers led to an estimation of the population-weighted Co–C bond lengths (2.019, 2.018, 2.025 and 2.020 Å, respectively), which do not differ very markedly from each other. However, the Co–C–C bond angles do differ quite markedly (121.0, 119.4, 122.2, 126.4°, respectively). With the results of Table 1 in mind, it seems possible that the measured $\Delta H^{\ddagger}$ at higher temperatures underestimates that near ambient temperature. Moreover, in the 'northern' and 'western' conformations, the Ado ligand represents a substantially larger steric barrier to acetamide side chain rotation than it does in either the 'eastern' and 'southern' conformations. This will result in a substantial decrease in the entropy of the ground state, which will be relieved as the transition state is approached. Hence, the entropic contribution to Co–C bond homolysis may increase with temperature. If these conjectures are correct, then the 9–12 orders of magnitude rate enhancement calculated for enzyme-abound AdoCbl may actually underestimate the rate enhancement brought about by the AdoCbl-dependent enzymes.

3.4. Coenzymatically-active analogues of adenosylcobalamin

Ado-13-epiCbl, in which the *e* side chain has been epimerized from the α face of the corrin ring, is a coenzymatically-active structural analogue of AdoCbl [80]. It fails to crystallize, and its structure was therefore examined by MM methods [81] (Fig. 5). Because the *e* side chain is pointed towards the β face of the molecule, the 'southern' conformation is destabilized, and the 'western' conformation is found to be the global minimum; three other conformations (a 'northern', a 'northeastern' and an 'eastern' conformation) are close in energy. When in the 'southern' conformation, the molecule is destabilized by some 6 kcal mol^{-1} relative to

AdoCbl in the same conformation; the *e* side chain and the adenine moiety moving away from each other, causing an opening of the Co–C–C bond angle.

There are many more nOe crosspeaks between Ado and non-Ado protons in the 13-epimer than in AdoCbl itself, indicative of the considerable conformational flexibility of this compound in solution. Using the crosspeaks assignments and measuring the relevant inter-proton distances in the MM structures suggests that all four conformations are populated in solution at ambient temperature. That 13-epi-AdoCbl is coenzymatically-active and the 'southern' conformation is apparently inaccessible, raises the question whether or not the active conformation of AdoCbl when bound to the protein in the AdoCbl-dependent enzymes is that observed crystallographically. We note with interest that in the recently-reported substrate-free structure of methylmalonyl coenzyme A mutase from *Propionibacterium shermanii* [82], the adenosyl ligand is in the northern conformation.

MM methods can be used to explore the feasibility of the synthesis of novel structures before costly and time-consuming synthetic endeavors are undertaken. This was done with an analog of AdoCbl, (α-ribo)AdoCbl, in which the Ado ligand is an α-*N*-glycoside rather than the usual β-*N*-glycoside [83]. Given that no

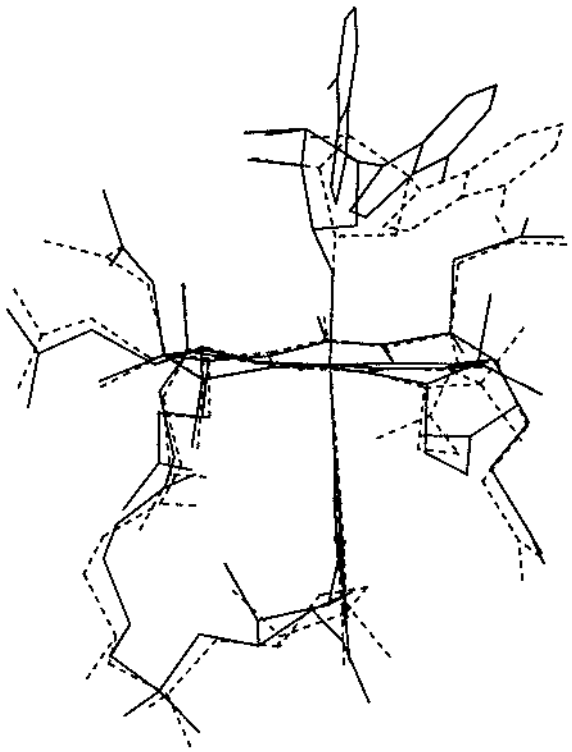

Fig. 6. Molecular structure of α-adenosylcobalamin predicted by molecular mechanics calculations (- - - - - -) and subsequently determined by single crystal X-ray diffraction (—). The disorder of the α-ado ligand in the solid state was modelled as originating from the contributions of two conformations.

structural parameters were unduly perturbed from their expected values and the strain energy was not significantly greater than that in AdoCbl itself, it was predicted that the compound should be stable with the same four locally-minimum conformations of the (α-ribo)Ado ligand as found for AdoCbl itself. The 'southern' conformation was predicted to be the global minimum, only 2.3 kcal mol^{-1} higher in energy than the 'southern' conformation of AdoCbl. The Co–C bond length and Co–C–C bond angle were predicted to be very similar to the values in AdoCbl.

The synthesis of the compound was duly successfully completed and the structure determination by X-ray diffraction methods confirmed the presence of the ligand over the southern quadrant of the corrin. The length of the Co–C bond and the value of the Co–C–C bond angle were indeed found to be very similar to that in AdoCbl. An unexpected finding was the disorder in the (α-ribo)Ado ligand, modeled when solving the structure as a distribution between two conformations. In the major conformation (0.57 occupancy), the adenine ring is virtually perpendicular to the corrin, while in the minor conformation, it is tilted downwards and is approximately halfway between its position in the major conformation and in AdoCbl itself (Fig. 6).

Once the structure was known, nOe-restrained MD simulations (see below) were used to explore the solution structure. At 300 K, the (α-ribo)Ado ligand is confined to the southern conformation, while the adenine ring was found to fluctuate from nearly parallel to virtually perpendicular to the corrin ring. Simulated annealing calculations yielded a collection of structures largely annealed into the southern conformation, but annealing into the other locally-minimum conformations predicted (Fig. 7) was also observed. Interestingly, the strain energy profile for the rotation of the ligand relative to the corrin ring (Fig. 7C) showed (unlike AdoCbl) quite substantial barriers to rotation away from the southern conformation. This explains why an nOe-restrained MD simulation at 300 K showed that only the southern conformation of this compound is populated at ordinary temperatures. Since (α-ribo)AdoCbl is a partially active coenzyme for the ribonucleotide reductase from *L. leichmanii*, this has raised discussion [83] about the conformation of the adenine ligand in the enzyme.

4. NOE-restrained molecular dynamics and simulated annealing calculations.

Molecular mechanics calculations are often carried out *in vacuo*. However, by coupling the technique to appropriate experimental information, simulations may be carried out on the solution structure. An example of this sort of information is the inter-proton distances that can be obtained from the strengths of the nuclear Overhauser effect (nOe) crosspeaks in 2D-NMR experiments. Information about the inter-proton distances is built into the simulations by adding a set of potential functions to restrain the H–H distances to values commensurate with the strength of the observed nOe crosspeaks. We have used simple parabolic functions of the form $E_{\mathrm{nOe}}(r_{i,j}) = k_{\mathrm{nOe}}(r_{ij} - r^{\circ}_{ij})$ where r_{ij} and r°_{ij} refer to the instantaneous and targeted H–H distance, respectively, and k_{nOe} is a restraining force constant. These

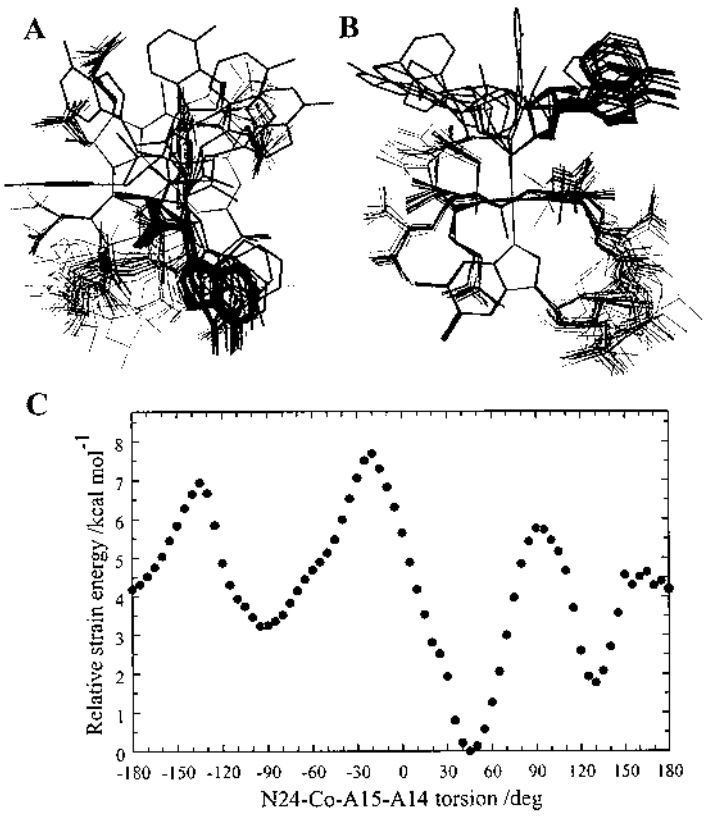

Fig. 7. The overlay from two different perspectives (A) from above; (B), from the C1–C19 bridge) of 27 annealed structures of (α-ribo)AdoCbl. The majority of the structures annealed into the global minimum, which is predicted, **C**, to be the 'southern' conformation. but other structures were also discovered. The relatively high barriers to rotation of the (α-ribo)adenosyl ligand (cf. Fig. 3) explains why an nOe-restrained MD simulation at 300 K showed that only this 'southern' conformation is populated.

force constants were determined by a modification of the procedure of Clore, et al. [84], who defined $k_{\mathrm{nOe}} = k_{\mathrm{B}}TS/2(\Delta_{ij}^{\pm})^2$ where k_{B} is the Boltzmann constant, T is the absolute temperature, S is a scaling factor and $\Delta_{ij}^{\pm}$ the positive and negative error estimates of r_{ij}. We have taken $S = 1$, $T = 300$ K and $\Delta_{ij}^{+} = \Delta_{ij}^{-}$. The crosspeaks were classified as strong, medium, weak or very weak [85–88] depending on whether they first appeared in a ROESY spectrum (at 500 or 600 MHz) at mixing times of 50, 100, 150 or 200 ms, respectively. The strength of an nOe crosspeak will depend both on the inter-proton distance and the relative orientations of the dipoles. Hence, strong, medium and weak NOEs are expected when, typically, $2.2 \leq r_{ij} \leq 2.7$ Å, $2.2 \leq r_{ij} \leq 3.4$ Å, and $2.2 \leq r_{ij} \leq 4.0$ Å, respectively. However, since the inter-proton distance is modeled by an harmonic function, it is usual [84] to expect r_{ij} for strong, medium and weak NOEs, respectively, to be $r_{ij} < 2.7$ Å, 2.7

Å $< r_{ij} <$ 3.4 Å, and 3.4 Å $< r_{ij} <$ 4.0 Å. We have used $r_{ij}^{o} < 2.5$, 3.0 and 4.0 Å for strong, medium, weak nOe's, respectively, and have also set $r_{ij}^{o} = 4.5$ Å for very weak nOe's. Clore, et al. [84] have used $\Delta_{ij}^{+} = \Delta_{ij}^{-} = 0.5$ Å, $\Delta_{ij}^{+} = 0.5$ Å and $_{ij}^{-} = 1.0$ Å, and $\Delta_{ij}^{+} = \Delta_{ij}^{-} = 1.0$ Å for a strong, medium and weak nOe, respectively. We took $\Delta_{ij}^{\pm} = 0.5$, 0.75, and 1.0 Å for the three cases, respectively, and $\Delta_{ij}^{\pm} = 2.0$ Å for a very weak nOe. At 300 K, therefore, the restraining force constant $k_{\mathrm{nOe}} = 1.2$, 0.52, 0.3 and 0.075 kcal mol^{-1} Å^{-2} for the four nOe classes, respectively. The inter-proton distance was taken to be violated when $r_{ij} = r_{ij}^{o} = \Delta_{ij}^{+}$ for strong and medium nOe's (i.e. at 3.0 and 3.8 Å, respectively), and then more rigorously as

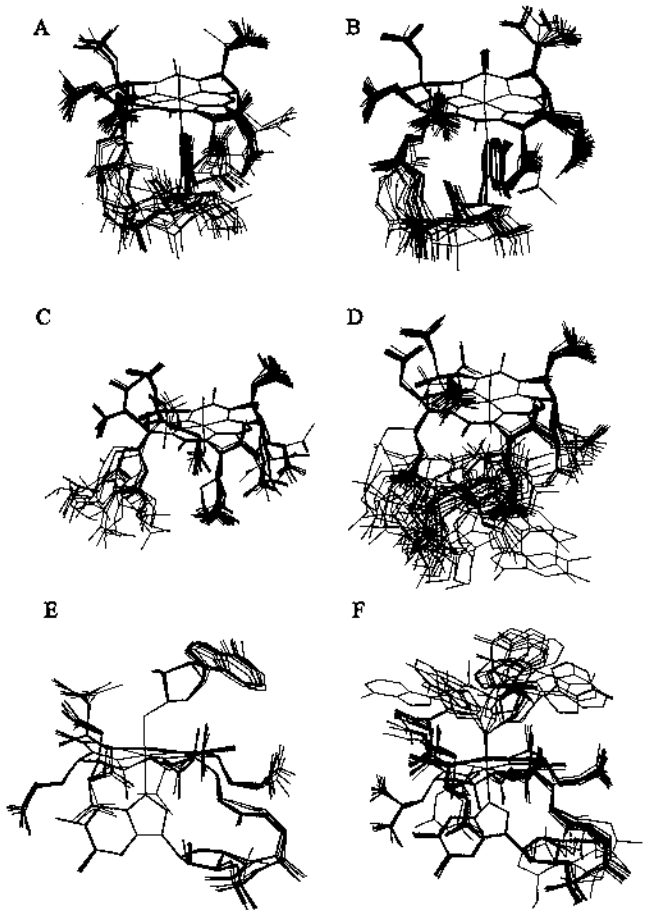

Fig. 8. Superposition (at the equatorial N atoms) of structures generated by molecular dynamics and simulated annealing procedures. (A) CH_3Cbl (25 structures); (B) CNCbl (25 structures); (C) CH_3Cbi^+ (25 structures); (D) $CH_3Me_3BzmCba^+$ (25 structures); (E) the 'southern' conformation of AdoCbl (8 structures shown, but 25 structures used to determine the consensus structure); and (F) the 'eastern' conformation of AdoCbl (20 structures shown, but 25 structures used to determine the consensus structure).

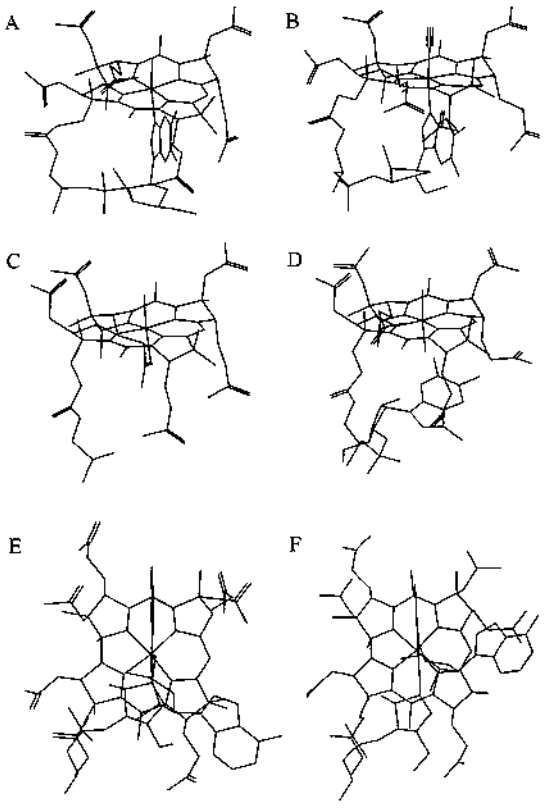

Fig. 9. Consensus structures of (A) CH_3Cbl; (B) CNCbl; (C) CH_3Cbi^+; (D) $CH_3Me_3BzmCba^+$; (E) the 'southern' conformation of AdoCb; and (F) the 'eastern' conformation of AdoCbl.

$r_{ij}^{o} = 0.8$ Å for the weak and very weak nOe', respectively (i.e. at 4.8 and 5.3 Å), since an nOe becomes essentially undetectable when $r_{ij} =$ ca. 5 Å [84].

Using this methodology, we have recently [89–91] studied the solution structures of methylcobalamin (CH_3Cbl), methylcobinamide (CH_3Cbi^+), cyanocobalamin (CNCbl), methyl- (3,5,6-trimethylbenzimidazolyl)cobamide ($CH_3Me_3BzmCba^+$, an analog of base-off methylcobalamin in which the N at the B3 position which coordinates Co in base-on cobalamins is methylated) and are currently exploring the solution structure of AdoCbl and $AdoCbi^+$. We assumed that CH_3Cbi^+ and $CH_3Me_3BzmCba^+$ were six-coordinate with H_2O in the α axial position. Some of the observations we have made are presented below. This should provide an indication of the sort of information that can be obtained from this methodology, but a full discussion in beyond the scope of the present paper.

The simulations with AdoCbl presented a particular problem. Since, at ambient temperature, both a 'southern' and an 'eastern' conformation are visited (Fig. 3), some of the observed nOe's are compatible with one but not the other. Preliminary

calculations involving molecular dynamics and simulated annealing procedures showed that if all nOe's are kept in position, the structure invariable annealed into a conformation half way between the two. Simulations were therefore performed with firstly, all nOe's compatible only with the 'eastern' conformation removed and secondly, those compatible with only the 'southern' conformation removed. The structures then predominantly annealed into the 'southern' and 'eastern' conformations, respectively.

Between 90 and 123 crosspeaks, not including those due to geminal hydrogens, could be resolved and assigned for the structures at the longest mixing time. The assignments of the pro-chiral protons were made by running a number of MD simulations of between 25 and 100 ps at 300 K, and changing the assignments until the minimum number of violations of the distance criteria was found. During a 300 ps MD simulation at 300 K with the inter-proton distances monitored every 10 fs, only 8.9, 8.8, 4.0, 2.3, 8.9 and 7.3% of the NOEs in CH_3Cbl, CNCbl, CH_3Cbi$^+$, CH_3Me_3BzmCba$^+$, the 'southern' conformation of AdoCbl and the 'eastern' conformation, respectively, showed a distance violation. Hence the MD-simulated structures were in good agreement with the experimental observations.

The average solution structure of each species was obtained by a molecular dynamics/simulated annealing procedure in which the system was heated from 0 to 1000 K over 5 ps, run at 1000 K for between 5 ps and 50 ps, cooled from 1000 to

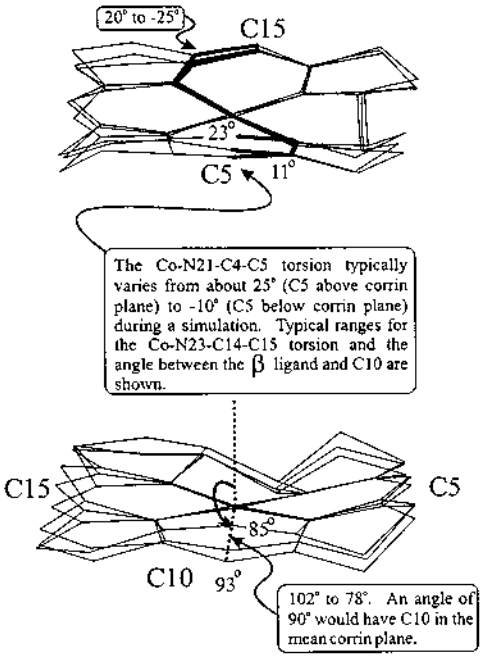

Fig. 10. The 'breathing motion' of the corrin ring, in which C5, C10 and C15 oscilliate from above to below the mean corrin plane.

300 K over 10 ps, and then energy-minimized. This was repeated 25 times for each species, and the overlay of the structures is shown in Fig. 8. The consensus structures were then obtained by averaging the coordinates of these 25 structures and energy-minimizing; they are shown in Fig. 9.

If all heavy atoms in the 25 structures of CH_3Cbl are superimposed with the heavy atoms of the consensus structure, the average r.m.s.d. is 1.21 ± 0.27 Å, whereas the average R.M.S.D. for the corrin ring atoms alone, when the structures were superimposed only at the corrin ring atoms, was 0.096 ± 0.026 Å. The analogous values for CNCbl were 0.66 ± 0.27 Å and 0.045 ± 0.024 Å; for CH_3Cbi^+, 1.39 ± 0.38 Å and 0.068 ± 0.023 Å; for $CH_3Me_3BzmCba^+$, 1.45 ± 0.61 Å and 0.066 ± 0.031 Å; for the 'southern' conformation of AdoCbl, 0.81 ± 0.18 Å and 0.058 ± 0.022 Å; and for the 'eastern' conformation of AdoCbl, 1.33 ± 0.54 Å and 0.059 ± 0.051 Å. In all cases, the major flexibility in the molecule is in the side-chains, or, in the case of the 'eastern' conformation of AdoCbl, in the orientation of the Ado ligand, rather than in the corrin ring itself. The flexibility of the corrin core increased in the order CNCbl < AdoCbl < $CH_3Me_3BzmCba^+$ ca. CH_3Cbi^+ < CH_3Cbl.

The tethering of the nucleotide loop to the metal does not impart upon it undue rigidity, and there is considerable variation in the disposition of the loop relative to the corrin ring in both CH_3Cbl and CNCbl (Fig. 8). The nucleotide loop spans a range of conformations, from an 'outward' conformation where, when the molecule is placed in its usual position and viewed directly from above, the C57–O58 carbonyl group points away from the molecule, in a southwesterly direction, to an 'inward' conformation, with the C57–O58 vector pointing southeasterly, and its extension intersecting that of the Co–C15 vector. In most crystal structures of cobalamins, the nucleotide loop is found in the 'inward' conformation; but at least one structure is known, that of 10-Cl-H_2OCbl [92], in which the nucleotide has crystallized in the 'outward' conformation.

The corrin ring undergoes a sort of 'breathing motion' (Fig. 10) in which C5, C10 and C15 oscillate from above to below the mean corrin plane. The extent of the breathing motion (as determined from the standard deviation of the torsional angles used to monitor the motion) increases in the order AdoCbl ('southern') < AdoCbl ('eastern') < CH_3Cbi^+ < CH_3Cbl < CNCbl < $CH_3Me_3BzmCba^+$, but there was no evidence of the motions being correlated; hence, despite $CH_3Me_3BzmCba^+$ undergoing apparently the biggest oscillations at these three corrin ring atoms, the overall folding of the ring, as measured by the corrin fold angle, was significantly smaller than for the cobalamins. In both the cobalamins and the cobinamides the B and C rings undergo greater distortions than the A and D rings and the 'eastern' portion of the molecule is more flexible than the 'western' portion; this is probably a consequence of the direct C1–C19 link in the western half. AdoCbl, in both conformations, is the least flexible structure examined; this is undoubtedly a consequence of the bulk Ado ligand restricting somewhat the vertical motions of the corrin ring.

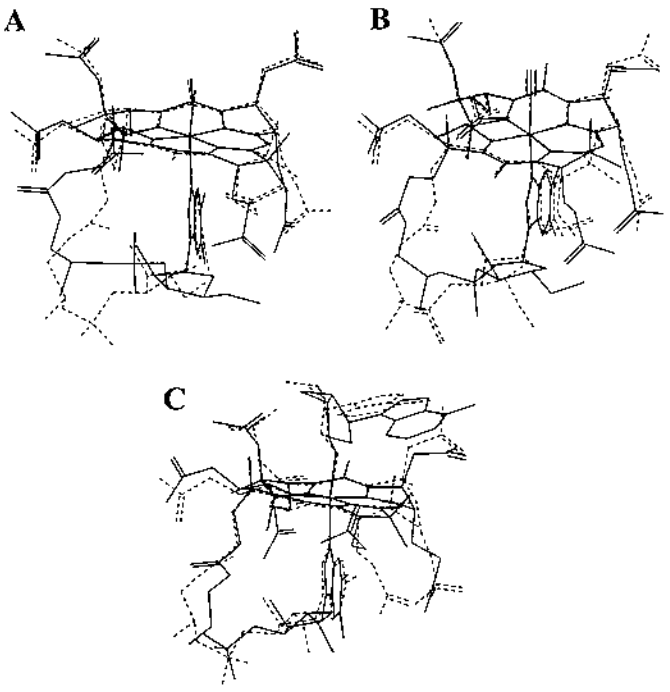

Fig. 11. Comparison of consensus structures (——) of cobalamins and their crystal structures (-----). (**A**) CNCbl; (**B**) CH_3Cbl; (**C**) AdoCbl (the 'southern' conformation).

The consensus structures of the three cobalamins are very similar to their crystal structures (Fig. 11), although the nucleotide loop is in a different conformation. The corrin fold angle has been defined [93] as the angle between the mean planes through N21, C4, C5, C6, N22, C9, C10, and N24, C16, C15, C14, N23, C11, C10, respectively. Alternatively, we define the ruffling angle (ruf angle) as the pseudo-angle C5–Co–C15. There is a reasonable correlation between the two (fold angle = $-2.00(11) \times$ ruf angle $+ 343(18)°$, $R^2 = 0.93$); the fold angle increases and the ruf angle decreases. The latter is a convenient measure of the former, and is readily measured during MD simulations, whereas the former, which requires least squares

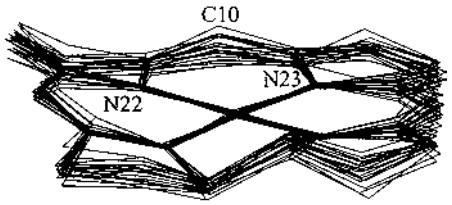

Fig. 12. The overlay of snapshots of the corrin core of CH_3Cbl during a molecular dynamics simulation at 300 K. The snapshots were captured during the simulation itself and do not represent energy-minimized structures. The view is from the C1–C19 bridge towards C10.

Table 3
Comparison of the corrin fold angle[a] and the ruf angle[b] in the consensus structures and their contributory structures as determined by molecular dynamics/simulated annealing calculations, and the crystal structures

Compound	Consensus structure		Contributory structures[i]		Crystal structure	
	Fold angle (°)	Ruf angle (°)	Fold angle (°)	Ruf angle (°)	Fold angle (°)	Ruf angle (°)
CH_3Cbl	16.8	162.3	16.4 ± 1.9(11.5–19.4)	163.4 ± 0.9(162–166)	158[c]	166.7
CNCbl	18.5	161.1	18.7 ± 1.5(15.7–21.2)	164.5 ± 0.7(162.9–166.1)	18.0[d]	164.7
AdoCbl ('southern')	13.5	165.2	13.9 ± 1.5(12.2–16.9)	164.5 ± 0.9(163.3–165.2)	14.8[e], 14.6,13.3,14.1f	166.2, 169.0, 167.7, 167.9[f]
CH_3Cbi^+	13.1	166.7	12.3 ± 1.8(9.5–16.0)	166.6 ± 0.6	–[g]	–
$CH_3Me_3^-BzmCba^+$	9.2	166.9	8.5 ± 0.4(3.4–11.8)	168.1 ± 0.6(166.9–169.4)	–[h]	–

[a] The angle between the mean planes through N21, C4, C5, C6, N22, C9, C10, and N24, C16, C15, C14, N23, C11, C10, respectively.
[b] The pseudo-angle C5–Co–C15.
[c] Ref. [55].
[d] Ref. [94].
[e] Ref. [56].
[f] Ref. [57]: neutron diffraction study, X-ray diffraction (molecule 1) and X-ray diffraction (molecule 2), respectively.
[g] Conformer not observed crystallographically.
[h] These compounds have yet to be successfully crystallized.
[i] (min.–max. values).

Table 4
The variation of the Corrin Ruf angle (and deduced variation in the Corrin fold angle) during a 300 ps molecular dynamics simulation at 300 K

Compound	Ruf angle		Fold angle[a]	
	Range	Mean(σ)	Range	Mean(σ)
CH3Cbl	151.2↔173.3	162.7(2.5)	41↔−4	17.6(5.0)
CNCbl	151.2↔172.6	164.0(2.5)	41↔−2	15.0(5.0)
$CH3Cbi^+$	154.2↔74.7	166.6(2.0)	35↔−6	9.8(4.0)
$CH3Me3BzmCba^+$	156.4↔175.0	167.3(2.4)	32↔−6	8.4(3.7)
AdoCbl('southern' conformation)	160.8↔167.8	164.7(0.5)	21↔7	13.6(2.0)
AdoCbl('eastern' conformation)	157.0↔171.2	164.1(1.2)	29↔1	14.8(4.8)

[a] Deduced from the ruf angle (see text).

fitting to two sets of atoms, is not. In Table 3, we compare the corrin fold angles and the ruf angles of the consensus structure, the 25 contributing structures and (where available), the crystal structures.

The fold of the consensus structure of the cobalamins is in all three cases very similar to that of the crystal structure. The two cobinamides are less folded. Clearly, the absence of the base in the α position allows for a more planar structure, and strongly suggests that base-on cobalamins are under steric strain.

Fairly lengthy (300 ps) molecular dynamics simulations at 300 K were performed to gain insight into the dynamic motion of the molecules. As an example, Fig. 12 shows the overlay of snapshots (only the corrin core is shown for clarity) taken during an MD simulation of CH_3Cbl at 300 K; the corrin ring is found to be highly flexible (Table 4). The mean fold angles of the two cobinamides is considerably smaller than that of the cobalamins, whilst, of the three cobalamins, AdoCbl is the least folded. This is undoubtedly a consequence of the bulky Ado ligand which restricts upward flexing of the corrin ring. Indeed, the 'eastern' conformation where the Ado ligand is in the vicinity of C10, and hence along the corrin fold axis, is more folded than the 'southern' conformation where the Ado ligand is closer to C15.

There is abundant crystallographic evidence that the corrin fold angle is significantly greater in the cobalamins than in the corrinoids lacking an axial nucleotide [91]; these MD studies confirmed for the first time the persistence of this effect in the cobinamides in solution. It has been suggested that the flexibility of the corrin ring is an important aspect of the coenzymatic function of AdoCbl [53,55,61,66–69,73,94–113]; in particular, the 'mechano-chemical trigger' mechanism [67–69,97,106,108,112,113] envisages the upward-flexing of the corrin ring, induced by a conformational change of the enzyme, sterically labilizing the Co–C bond in the β coordination site. The MM modelling work suggests that the corrin is indeed flexible enough for such a mechanism, and this question is currently being addressed.

5. Future prospects

With the crystal structures of enzyme-bound cobalamins beginning to emerge [22,84,114], there is a realistic possibility of modelling these species in the future. Performing molecular dynamics simulations will, in particular, offer the possibility of gaining insight into factors that control the structure of enzyme-bound cobalamins. A force field specifically developed for modeling proteins, such as the AMBER force field [14–16] will be required. Work is currently underway in translating the MM2 force field for the cobalamins to AMBER.

Acknowledgements

Much of the work described was funded by the Foundation for Research Development, Pretoria, South Africa (H.M.M.), the University of the Witwatersrand (H.M.M.) and the National Institute of General Medical Sciences (grant GM 48858 to K.L.B.).

References

[1] U. Burkert, N.L. Allinger, Molecular Mechanics. In: ACS Monograph, vol. 177, American Chemical Society, Washington, DC, 1982.
[2] A.R. Leach, Molecular Modelling: Principles and Applications, Longman, Harlow, Essex, UK, 1996.
[3] B.P. Hay, Coord. Chem. Rev. 126 (1993) 177.
[4] P. Comba, T.W. Hambley, Molecular Modeling of Inorganic Compounds, VCH, New York, 1995.
[5] M. Zimmer, Chem. Rev. 95 (1995) 2629.
[6] (a) C.L. Landis, D.M. Root and T. Cleveland, in: D.B. Boyd and K.B. Lipkowitz (Eds.), Reviews in Computational Chemistry, vol. 6, VCH, New York, 1995, p. 63. (b) C.R. Landis, T.K. Firman, T. Cleveland and D.M. Root, NATO ASI Ser. Ser. 3(41) (1997) 49.
[7] L.J. Bartolotti and L.G. Pedersen, Pract. Appl. Comput. Aided Drug Des. (1997) 471.
[8] P. Comba, in: W. Gans, A. Amann, J.C.A. Boeyens (Eds.), Fundamental Principles of Molecular Modeling, Plenum, New York, 1996, p. 167.
[9] P. Kollman, in: R.L. Orenstein (Ed.), Biomarcomolecules: 3-D Applications (34th Hanford Symposium on Health and the Environment), Batelle Press, Columbus, Ohio, 1997, p. 21.
[10] (a) R.J. Deeth and V.J. Paget, J. Chem. Soc. Dalton Trans. (1997) 527. (b) R.J. Deeth, I.J. Munslow, V.J. Paget, NATO ASI Ser. Ser. 3, 41 (1997) 77.
[11] N.L. Allinger, Adv. Phys. Org. Chem. 13 (1976) 1.
[12] N.L. Allinger, J. Am. Chem. Soc. 99 (1977) 8127.
[13] N.L. Allinger, Y.H. Yuh, J.H. Lii, J. Am. Chem. Soc. 111 (1989) 8551.
[14] S.J. Weiner, P.A. Kollman, D.A. Case, U.C. Singh, C. Ghio, G. Alagona, S. Profeta, P.J. Weiner, J. Am. Chem. Soc. 106 (1984) 765.
[15] S.J. Weiner, P.A. Kollman, D.T. Nguyen, D.A. Case, J. Comput. Chem. 7 (1986) 230.
[16] W.D. Cornell, P. Ciepalk, C.I. Bayley, I.R. Gould, K.M. Merz, D.M. Ferguson, D.C. Spellmeyer, T. Fox, J.W. Caldwell, P.A. Kollman, J. Am. Chem. Soc. 117 (1995) 5179.
[17] W.L. Jorgensen, J. Tirado-Rives, J. Am. Chem. Soc. 110 (1988) 1657.
[18] J. Pranate, S. Wierschke, W.L. Jorgensen, J. Am. Chem. Soc. 113 (1991) 2810.

[19] B.R. Brooks, R.E. Bruccoleri, B.D. Olafson, D.J. States, S. Swaminathan, M.J. Karplus, J. Comput. Chem. 4 (1983) 187.
[20] E.-I. Ochiai, in: H. Sigel, A. Sigel (Eds.), Metal Ions in Biological Systems, vol. 30, Marcel Dekker, New York, 1994, p. 255.
[21] B.T. Golding, R.J. Anderson, S. Ashwell, C.H. Edwards, I. Garnett, F. Kroll, W. Buckel, in: B. Kräutler, D. Arigoni, B.T. Golding (Eds.), Vitamin B12 and B12-Proteins, Wiley-VCH, Weinheim, 1998, p. 201.
[22] M. Rossi, J.P. Glusker, in: J.F. Liebman, A. Greenberg (Eds.), Environmental Influences and Recognition in Enzyme Chemistry, VCH, New York, 1988, p. 1.
[23] J.R. Guest, S. Friedman, D.D. Woods, E.L. Smith, Nature 195 (1962) 340.
[24] C.L. Drennan, M.M. Dixon, D.M. Hoover, J.T. Jarrett, C.W. Goulding, R.G. Matthews, M.L. Ludwig, in: B. Kräutler, D. Arigoni, B.T. Golding (Eds.), Vitamin B12 and B12-Proteins, Wiley-VCH, Weinheim, 1998, p. 133.
[25] R.T. Taylor, in: D. Dolphin (Ed.), B_{12}, vol. 2, Wiley, New York, 1982, p. 307.
[26] B.A. Blylock, T.C. Stadtman, Biochem. Biophys. Res. Commun. 11 (1963) 34.
[27] J.M. Poston, K. Kuratomi, E.R. Stadtman, Ann. N.Y. Acad. Sci. 112 (1964) 804.
[28] A.K. Rappé, C.J. Casewit, K.S. Colwell, W.A. Goddard, W.M. Skiff, J. Am. Chem. Soc. 114 (1992) 10024.
[29] V.S. Allured, C.M. Kelley, C.R. Landis, J. Am. Chem. Soc. 113 (1991) 1.
[30] P.V. Bernhardt, P. Comba, Inorg. Chem. 31 (1992) 2638.
[31] J.E. Bol, C. Buning, P. Comba, J. Reedijk, M. Ströhle, J. Comput. Chem. 19 (1998) 512.
[32] D.L. Kepert, Inorganic Stereochemistry, Springer, Berlin, 1982.
[33] M.C. Favas, D.L. Kepert, Prog. Inorg. Chem. 28 (1982) 309.
[34] A.M. Bond, T.W. Hambley, D.R. Mann, M.R. Snow, Inorg. Chem. 26 (1987) 2257.
[35] B.P. Hay, Inorg. Chem. 30 (1991) 2876.
[36] D.M. Ferguson, D.J. Raber, J. Comput. Chem. 11 (1990) 1061.
[37] R.D. Hancock, G.J. McDougall, J. Am. Chem. Soc. 102 (1980) 6511.
[38] G.R. Brubaker, D.W. Johnson, Inorg. Chem. 23 (1984) 1591.
[39] A. Vedani, M. Dobler, J.D. Dunitz, J. Comput. Chem. 7 (1986) 701.
[40] M.G.B. Drew and D.G. Nicholson, J. Chem. Soc. Dalton Trans. (1986) 1543.
[41] M. Zimmer, R.H. Crabtree, J. Am. Chem. Soc. 112 (1990) 1062.
[42] O.Q. Munro, J.C. Bradley, R.D. Hancock, H.M. Marques, F. Marsicano, P.W. Wade, J. Am. Chem. Soc. 114 (1992) 7218.
[43] H.M. Marques, O.Q. Munro, N.E. Grimmer, D.C. Levendis, F. Marsicano, G. Pattrick, T. Markoulides, J. Chem. Soc. Faraday Trans. 91 (1995) 1741.
[44] O.Q. Munro, H.M. Marques, P.G. Debrunner, K. Mohanrao, W.R. Scheidt, J. Am. Chem. Soc. 117 (1995) 935.
[45] R.D. Hancock, J.S. Weaving and H.M. Marques, J. Chem. Soc. Chem. Commun. (1989) 1176.
[46] H.M. Marques, K.L. Brown, J. Mol. Struct. (Theochem) 340 (1995) 97.
[47] H.M. Marques, C. Warden, M. Monye, M.S. Shongwe, K.L. Brown, Inorg. Chem. 37 (1998) 2578.
[48] HYPERCHEM, Tools for Molecular Modeling, V. 5.1, Hyperchem, Gainesville, FL, USA.
[49] H. Stoeckli-Evans, E. Edmond, D.C. Hodgkin, J. Chem. Soc. Perkin Trans. 2 (1972) 602.
[50] K.L. Brown, D.R. Evans, J.D. Zubkowski, E.J. Valente, Inorg. Chem. 35 (1996) 415.
[51] K.L. Brown, X. Zou, G.-Z. Wu, J.D. Zubkowski, E.J. Valente, Polyhedron 14 (1995) 1621.
[52] A. Bax, L.G. Marzilli, M.F. Summers, J. Am. Chem. Soc. 109 (1987) 566.
[53] N. Bresciani-Pahor, M. Forcolin, L.G. Marzilli, L. Randaccio, M.F. Summers, P.J. Toscano, Coord. Chem. Rev. 63 (1985) 1.
[54] H.M. Marques, K.L. Brown, Inorg. Chem. 34 (1995) 3733.
[55] M. Rossi, J.P. Glusker, L. Randaccio, L.G. Marzilli, J. Am. Chem. Soc. 107 (1985) 1729.
[56] P.G. Lenhert, Proc. R. Soc. Lond. Ser. A 303 (1968) 45.
[57] H.F.L. Savage, P.F. Lindley, J.L. Finney, P.A. Timmins, Acta Crystallogr. B 43 (1987) 280.
[58] B.D. Martin, R.G. Finke, J. Am. Chem. Soc. 112 (1990) 2419.
[59] B.D. Martin, R.G. Finke, J. Am. Chem. Soc. 114 (1992) 585.
[60] B.P. Hay, R.G. Finke, Polyhedron 7 (1988) 1469.

[61] K.L. Brown, H. Brooks, Inorg. Chem. 30 (1991) 3420.
[62] K.L. Brown, D.R. Evans, Inorg. Chem. 33 (1994) 6380.
[63] Y. Toraya, R.L. Blakely, Biochemistry 12 (1973) 24.
[64] S.M. Chemaly and J.M. Pratt, J. Chem. Soc. Dalton Trans. (1980) 2259.
[65] J.M. Pratt, J. Mol. Catal. 23 (1984) 187.
[66] Y. Toraya, T. Matsumoto, M. Ichikawa, Y. Itah, T. Sugawara, Y. Mizuno, J. Biol. Chem. 261 (1986) 9289.
[67] G.N. Schrauzer, J.H. Grate, J. Am. Chem. Soc. 103 (1981) 541.
[68] J. Halpern, Science 227 (1985) 869.
[69] J.H. Grate, G.N. Schrauzer, J. Am. Chem. Soc. 101 (1979) 6401.
[70] B.P. Hay, R.G. Finke, J. Am. Chem. Soc. 108 (1987) 4820.
[71] J.D. Brodie, Proc. Natl. Acad. Sci. USA 62 (1969) 461.
[72] S.-H. Kim, H.L. Chen, N. Feilchenfeld, J. Halpern, J. Am. Chem. Soc. 110 (1988) 3120.
[73] M.D. Waddington, R.G. Finke, J. Am. Chem. Soc. 115 (1993) 4629.
[74] K.L. Brown, H.B. Brooks, D. Behnke, D.W. Jacobsen, J. Biol. Chem. 226 (1991) 6737.
[75] K.L. Brown, X. Zou, D.R. Evans, Inorg. Chem. 33 (1994) 5713.
[76] K.L. Brown, S. Cheng, H.M. Marques, Inorg. Chem. 34 (1995) 3038.
[77] S. Saebo, L. Radom, H.F. Schaefer, J. Chem. Phys. 78 (1983) 845.
[78] K.L. Brown, S. Cheng, J.D. Zubkowski, E.J. Valente, Inorg. Chem. 36 (1997) 1772.
[79] K.L. Brown, H.M. Marques, Polyhedron 15 (1996) 2187.
[80] T. Toraya, T. Shirakashi, S. Fukui, H.P.C. Hogenkamp, Biochemistry 14 (1975) 3949.
[81] K.L. Brown, S. Cheng, H.M. Marques, Polyhedron 17 (1998) 2213.
[82] F. Mancia, P.R. Evans, Structure 6 (1998) 711.
[83] K.L. Brown, S. Cheng, X. Zou, J. Li, G. Chen, E.J. Valente, J.D. Zubkowski, H.M. Marques, Biochemistry 37 (1998) 9704.
[84] G.M. Clore, A.T. Brünger, M. Karplus, A.M. Gronenborn, J. Mol. Biol. 191 (1986) 523.
[85] W. Braun, G. Wider, K.H. Lee, K. Wüthrich, J. Mol. Biol. 169 (1983) 921.
[86] M.P. Williamson, T.F. Havel, K. Wüthrich, J. Mol. Biol. 182 (1985) 295.
[87] G.M. Clore, A.M. Gronenborn, A.T. Brünger, M. Karplus, J. Mol. Biol. 185 (1985) 435.
[88] G.M. Clore, A.M. Gronenborn, Science 252 (1991) 1390.
[89] H.M. Marques, R.P. Hicks, and K.L. Brown, J. Chem. Soc. Chem. Commun. (1996) 1427.
[90] H.M. Marques and K.L. Brown, J. Mol. Struct. (1999) in press.
[91] K.L. Brown, X. Zou, H.M. Marques, J. Mol. Struct. (Theochem) 453 (1998) 209.
[92] K.L. Brown, S. Cheng, X. Zou, J.D. Zubkowski, E.J. Valente, L. Knapton, H.M. Marques, Inorg. Chem. 36 (1997) 3666.
[93] J.P. Glusker, in: D. Dolphin (Ed.), B_{12}, vol. 1, Wiley, New York, 1982, p. 3.
[94] B. Kräutler, R. Konrat, E. Stupperich, G. Fäber, K. Gruber, C. Kratky, Inorg. Chem. 33 (1994) 4128.
[95] H.A.O. Hill, J.M. Pratt, R.J.P. Williams, Chem. Br. 5 (1969) 156.
[96] B.M. Babior, Acc. Chem. Res. 8 (1975) 376.
[97] T. Toraya, E. Krodel, A.S. Mildvan, R.H. Abeles, Biochemistry 18 (1979) 417.
[98] S.M. Chemaly and J.M. Pratt, J. Chem. Soc. Dalton Trans. (1980) 2274.
[99] L. Randaccio, N. Bresciani-Pahor, P.J. Toscano, L.G. Marzilli, J. Am. Chem. Soc. 103 (1981) 6347.
[100] J.M. Pratt, in: D. Dolphin (Ed.), B_{12}, vol. 1, Wiley, New York, 1982.
[101] J. Halpern, Pure Appl. Chem. 55 (1983) 1059.
[102] D.W. Christianson, W.N. Lipscomb, J. Am. Chem. Soc. 107 (1985) 2682.
[103] T. Toraya, N. Watanabe, M. Ichikawa, T. Matsumoto, K. Ushido, S. Fukui, J. Biol. Chem. 262 (1987) 8544.
[104] M.K. Geno, J. Halpern, J. Am. Chem. Soc. 109 (1987) 1236.
[105] B.P. Hay, R.G. Finke, J. Am. Chem. Soc. 109 (1987) 8012.
[106] V.B. Pett, M.N. Liebman, P. Murray-Rust, K. Prasad, J.P. Glusker, J. Am. Chem. Soc. 109 (1987) 3207.

[107] L. Zhu, N.M. Kostíc, Inorg. Chem. 26 (1987) 4194.
[108] T. Toraya, A. Ishida, Biochemistry 27 (1988) 7677.
[109] J. Halpern, Bull. Soc. Chim. Fr. (1988) 187.
[110] L. Randaccio, N. Bresciani-Pahor, E. Zangrando, L.G. Marzilli, Chem. Soc. Rev. 18 (1989) 225.
[111] I. Sagi, M.R. Chance, J. Am. Chem. Soc. 114 (1992) 8061.
[112] J.M. Pratt, Pure Appl. Chem. 65 (1993) 1513.
[113] L.G. Marzilli, in: J. Reedijk (Ed.), Bioinorganic Chemistry, Marcel Dekker, New York, 1993, p. 227.
[114] F. Mancia, N.H. Keep, A. Nakagawa, P.F. Leadley, S. McSweeney, B. Rasmussen, P. Bösecke, O. Diat, P.R. Evans, Structure 4 (1996) 339.